

# Spectra and femtoscopic scales in a hydrokinetic model for baryon-rich fireballs

Iu.A. Karpenko <sup>a</sup>, A.S. Khvorostukhin <sup>b,c,e</sup>, Yu.M. Sinyukov <sup>a,d</sup>,  
V.D. Toneev <sup>b,e</sup>

<sup>a</sup>*Bogolyubov Institute of Theoretical Physics, 03680 Kiev-143, Ukraine*

<sup>b</sup>*Joint Institute for Nuclear Research, 141980 Dubna, Moscow Region, Russia*

<sup>c</sup>*Institute of Applied Physics, Moldova AS, MD-2028 Kishineu, Moldova*

<sup>d</sup>*ExtreMe Matter Institute EMMI, GSI Helmholtzzentrum für  
Schwerionenforschung GmbH, 64291 Darmstadt, Germany*

<sup>e</sup>*GSI Helmholtzzentrum für Schwerionenforschung GmbH, D-64291 Darmstadt,  
Germany*

---

## Abstract

The hydrokinetic model and the scheme of dynamical freeze out proposed earlier for the RHIC energy are extended to lower colliding energy for non-vanishing baryon chemical potential. In this case a new two-phase equation of state is applied where baryon-rich hadronic matter is described within modified relativistic mean-field theory. As an example, the approach is employed for analyzing pion and kaon spectra and interferometry radii of Pb+Pb collisions at laboratory energies 40 and 158 AGeV. A good agreement is observed for the transverse mass dependence of the longitudinal radius for both energies studied. The transverse radii  $R_{out}, R_{side}$  reproduce experiment at  $E_{lab} = 158$  AGeV but at  $E_{lab} = 40$  AGeV there is a marked (20 %) difference from experimental points. This discrepancy is more noticeable in analysis of the ratio  $R_{out}/R_{side}$ . Nevertheless, considered examples of application of the hydrokinetic model with equation of state including the first order phase transition are quite successful and further development of the model is required.

---

## 1 Introduction

An analysis of the experimental data in nucleus-nucleus collisions obtained at Relativistic Heavy Ion Collider(RHIC) [1] and very recently at Large Hadron Collider (LHC) [2] denotes hydrodynamics as an adequate tool to describe a behavior of the bulk of the matter created at these collisions. The reason could

be that the collective behavior of the quark-gluon plasma at the reached temperatures is similar to what an almost perfect fluid has. The hydrodynamic models use then the thermodynamic equation of state (EoS) reconciled with the Lattice QCD. The successful description of RHIC data within hydrodynamic approaches with artificial sharp freeze-out [3] as well as with dynamical freeze-out in the HydroKinetic Model (HKM) [4,5,6] were done and the predictions for the spectra and femtoscales at LHC are in quite reasonable agreement [2,3,7].

As for the applicability of hydrodynamic approach to lower energies, such as the SPS ones and planning experiments NICA and FAIR, it is a questionable issue. First, as expected, created fireballs spend only small part of its lifetime if any in quark-gluon phase. An evolution of the hadronic matter could be non-equilibrated, neither thermally, nor chemically. Since in the HKM model [4] the evolution and gradual decay of the hadronic matter are described as non-equilibrated process, it seems reasonable to try to apply this model to relatively small collision energies. It is the main aim of our work.

One of the crucial points is the equation of state at large baryonic chemical potentials, which are typical for these energies. As known, because of the principal technical problem the EoS cannot be found from the lattice QCD calculations at large baryonic chemical potentials. Currently such an estimate should be obtained rather from a detailed study of strongly interacting hadronic matter supplemented by the model of quark-gluon phase at large  $\mu_B$  and  $\mu_S$ . In this paper we will use the EoS taking into account a possible phase transition between quarks-gluons and hadrons including in-medium modification of hadron properties in hot and dense nuclear surrounding [8]

## 2 Basic features of the model

Let us briefly describe the main features of the HKM [5,6]. It incorporates hydrodynamical expansion of the systems formed in  $A+A$  collisions and their dynamical decoupling described by escape probabilities. The basic hydro-kinetic code includes decays of resonances into expanding hadronic chemically non-equilibrated system and, based on the resulting composition of the hadron-resonance gas at each space-time point, provides the equation of state (EoS) in a vicinity of this point. The obtained local EoS allows one to determine the further evolution of the considered fluid elements. The complete picture of the physical processes in central Pb + Pb collisions encoded in calculations is the following.

## 2.1 Initial conditions

Our results are all related to the central rapidity slice where we use the boost-invariant Bjorken-like initial condition. We consider the proper time of thermalization of quark-gluon matter as the minimal one discussed in the literature,  $\tau_0 = 1$  fm/c. The initial energy density in the transverse plane is supposed to be Glauber-like [9], i.e. is proportional to the participant nucleon density for Pb+Pb (SPS) and Au+Au (RHIC, LHC) collisions with zero impact parameter. The height of the distribution - the maximal initial energy density  $\epsilon(r=0) = \epsilon_0$  is a fitting parameter. Also, at time  $\tau_i$ , there is peripheral region with relatively small initial energy densities:  $\epsilon(r) < 0.5$  GeV/fm<sup>3</sup>. This part of the matter ("corona") have no chance to be involved in thermalization process [10]. Thus, it should be considered separately from the thermal bulk of the matter and should not include it in hydrodynamic evolution. By itself the corona gives no essential contribution to the hadron spectra for central collisions [10].

At the time of thermalization,  $\tau_0 = 1$  fm/c, the system has already developed collective transverse velocities [11,12]. The initial transverse rapidity profile is supposed to be linear in transverse radius  $r_T$ :

$$\eta_T = \alpha \frac{r_T}{R_T} \quad \text{where} \quad R_T = \sqrt{\langle r_T^2 \rangle}. \quad (1)$$

Here  $\alpha$  is a second fitting parameter. Note that the fitting parameter  $\alpha$  should also include a positive correction for underestimated resulting transverse flow since in this work we do not take directly into account viscosity effects [13] neither at the QGP stage nor at hadronic one. In HKM formalism [5] viscosity effects at the hadronic stage are incorporated in mechanisms of the back reaction of particle emission in hydrodynamic evolution which we ignore in current calculations. Since the corrections to transverse flows which depend on unknown viscosity effects are unknown, we use a fitting parameter  $\alpha$  to describe the "additional unknown portion" of flows, caused by three factors: development of the pre-thermal flows, viscosity effects in quark-gluon plasma and in addition event-by-event fluctuations of the initial conditions. The latter also leads to an increase of the "effective" transverse flows, obtained by averaging at the final stage, as compared to the results based on the initial conditions averaged over initial fluctuations [14]. Since we use the last type of initial conditions, it should also lead to an increase of the effective parameter  $\alpha$ .

## 2.2 Equation of state

We match the equation of state at the point of the chemical freeze out  $T_{ch}$  which separates chemically equilibrated and non-equilibrated thermodynamic zones. As to the chemically equilibrated region  $T > T_{ch}$  the EoS is constructed on the basis of the modified relativistic mean-field model with Scaled Hadron Masses and Couplings (SHMC) [8,15]. In this SHMC model the Lagrangian density of hadronic matter is a sum of several terms:

$$\mathcal{L} = \mathcal{L}_{\text{bar}} + \mathcal{L}_{\text{MF}} + \mathcal{L}_{\text{ex}} . \quad (2)$$

The Lagrangian density of the baryon component interacting via  $\sigma, \omega$  mean fields is as follows:

$$\mathcal{L}_{\text{bar}} = \sum_{b \in \{\text{bar}\}} \left[ i \bar{\Psi}_b \left( \partial_\mu + i g_{\omega b} \chi_\omega \omega_\mu \right) \gamma^\mu \Psi_b - m_b^* \bar{\Psi}_b \Psi_b \right] . \quad (3)$$

The considered baryon set  $\{b\}$  consists of all baryons and low-lying resonances with the mass  $m_b < 1700$  MeV, including strange and double-strange hyperons as well as antiparticles. The used  $\sigma$ -field dependent effective masses of baryons are [8,15,16]

$$m_b^*/m_b = \Phi_b(\chi_\sigma \sigma) = 1 - g_{\sigma b} \chi_\sigma \sigma / m_b , \quad b \in \{b\} . \quad (4)$$

In Eqs. (3), (4)  $g_{\sigma b}$  and  $g_{\omega b}$  are coupling constants and  $\chi_\sigma(\sigma)$ ,  $\chi_\omega(\sigma)$  are coupling scaling functions.

The  $\sigma$ -,  $\omega$ -meson mean field contribution is given by

$$\begin{aligned} \mathcal{L}_{\text{MF}} &= \frac{\partial^\mu \sigma \partial_\mu \sigma}{2} - \frac{m_\sigma^{*2} \sigma^2}{2} - U(\chi_\sigma \sigma) - \frac{\omega_{\mu\nu} \omega^{\mu\nu}}{4} + \frac{m_\omega^{*2} \omega_\mu \omega^\mu}{2} , \quad (5) \\ \omega_{\mu\nu} &= \partial_\mu \omega_\nu - \partial_\nu \omega_\mu , \quad U(\chi_\sigma \sigma) = m_N^4 \left( \frac{b}{3} f^3 + \frac{c}{4} f^4 \right) , \quad f = g_{\sigma N} \chi_\sigma \sigma / m_N . \end{aligned}$$

There exist only  $\sigma$  and  $\omega_0$  mean field solutions of equations of motion. The mass terms of the mean fields are

$$m_m^*/m_m = |\Phi_m(\chi_\sigma \sigma)| , \quad \{m\} = \sigma, \omega . \quad (6)$$

The dimensionless scaling functions  $\Phi_b$  and  $\Phi_m$ , as well as the coupling scaling functions  $\chi_m$ , depend on the scalar field in combination  $\chi_\sigma(\sigma) \sigma$ . Following

[16] we assume approximate validity of the Brown-Rho scaling ansatz in the simplest form

$$\Phi = \Phi_N = \Phi_\sigma = \Phi_\omega = \Phi_\rho = 1 - f. \quad (7)$$

The third term in the Lagrangian density (2) corresponds to meson quasiparticle excitations, where particles with  $m_m < 1100$  MeV are included. The choice of parameters and other details of the SHMC model can be found in [8,15].

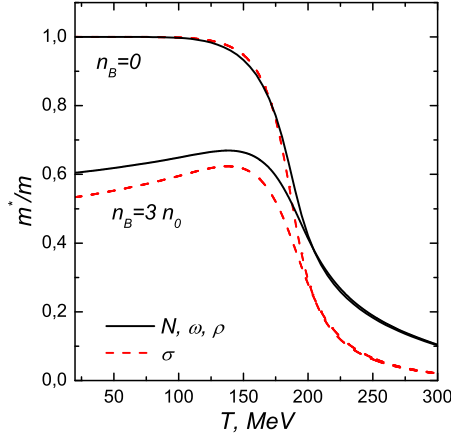


Fig. 1. The temperature dependence of effective masses of the nucleon,  $\omega$  and  $\rho$  excitations (solid line) and of the  $\sigma$ -meson excitation (dashed line) calculated within the SHMC model for two values of the baryon density  $n_B$ .

Within SHMC model different thermodynamical quantities in thermal equilibrium hadron matter are calculated at fixed temperature  $T$  and baryon chemical potential  $\mu_B$ . In Fig.1 the  $T$  and  $\mu_B$  dependence of hadron masses is pictured. Note that these masses sharply decrease in the vicinity of the expected phase transition and thereby affect on the fireball evolution.

The quark-gluon plasma phase is treated in the conventional quark bag model with massive quark and gluons. A two-phase model allowing for the first order phase transition from the hadron phase (H) to the strongly coupled quark gluon plasma (Q) is constructed by means of the Gibbs conditions. These are conditions for thermal ( $T^Q = T^H$ ), mechanical ( $P^Q = P^H$ ) and chemical ( $\mu_B^Q = \mu_B^H$ ,  $\mu_{\text{str}}^Q = \mu_{\text{str}}^H$ ) equilibrium.

There is a reasonable agreement of our two-phase thermodynamics with available QCD lattice calculations [8,15]. For  $\mu_B = 0$  some discrepancy is seen in energy density near the critical temperature  $T_c$  due to the fact that by construction we have the first order phase transition while in lattice calculations we deal with a sharp crossover-type transition. The colliding energies of interest are below an anticipated critical point and the first order phase transition

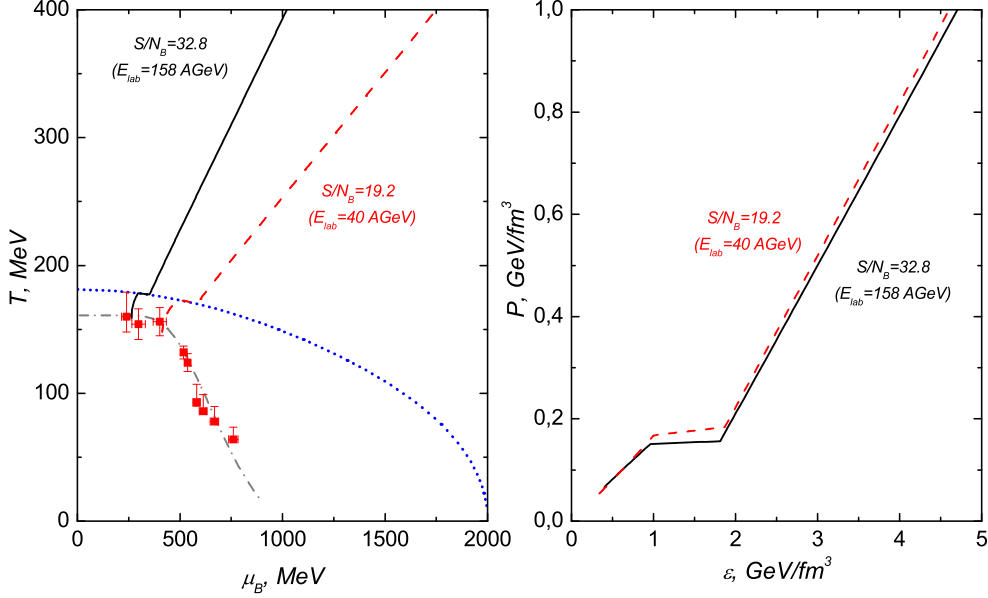


Fig. 2. *Left panel:* Isoentropic trajectories in the  $T - \mu_B$  plane for two values of entropy-to-baryon number ratio. The quark-hadron phase boundary [15] and the freeze out curve [17] are shown by the dotted and dashed dash-dashed lines, respectively. Experimental points are from review article [17]. *Right panel:* Equation of state within two-phase model for the same values of the entropy baryon number ratio as in the left panel.

is expected. Unfortunately, there is no lattice data for these large  $\mu_B$  range. In the left panel of Fig.2 we demonstrate isoentropic trajectories for two fixed ratios of entropy  $S$  to baryon number  $N_B$ ,  $S/N_B = 19.2$  and  $32.8$ , corresponding to that of an expanding fireball at  $E_{lab} = 40$  and  $158$  AGeV. When a trajectory reaches the phase boundary it is flattening in accordance with the mixed phase of the Maxwell construction in the two-phase model (see the right panel in Fig.2). Assuming chemical equilibrium our hydrodynamics is used till the chemical freeze out curve shown in Fig.2 by the dotted line. At temperature below  $T_{ch}$  we apply non-equilibrium treatment.

The EoS for baryon-rich fireballs described above is used up to the temperature of the chemical equilibrium  $T_{ch}$ . We should match this chemically equilibrated region  $T > T_{ch}$  and non-equilibrated hadronic region at  $T < T_{ch}$ . The last is described in the HKM as an ideal gas of hadrons and their resonances in correspondence with the concept of chemical freeze-out. We fix the chemical freeze-out temperature and baryon chemical potential to be  $\{T, \mu_B\} = \{160 \text{ MeV}, 220 \text{ MeV}\}$  for  $E_{Lab} = 158$  GeV collisions and  $\{T, \mu_B\} = \{148 \text{ MeV}, 370 \text{ MeV}\}$  for  $E_{Lab} = 40$  GeV collisions, based on  $T_{ch}(\sqrt{s_{NN}})$ ,  $\mu_B(\sqrt{s_{NN}})$  parameterizations obtained from particle number ratio analysis performed in [19]. In both cases, strange chemical potential is calculated from the condition of zero strange density. The proper choice of  $T_{ch}$  and  $\mu_B$  guar-

antees us the correct particle number ratios for all quasi-stable particles (here we calculate only pion and kaon observables). Below  $T_{ch}$  a composition of the hadron gas is changed only due to resonance decays into expanding fluid. We include  $N_h = 326$  well-established hadron states made of  $u$ ,  $d$ ,  $s$ -quarks with masses up to 2.6 GeV from PDG table [18], as well as the most possible decay channels of them. The EoS in this chemically non-equilibrated system depends now on particle number densities  $n_i$  of all the  $N_h$  particle species  $i$ :  $p = p(\epsilon, \{n_i\})$ . Since the energy densities in expanding system do not directly correlate with resonance decays, all the variables in the EoS depend on space-time points and so an evaluation of the EoS is incorporated in the hydrodynamic code. We calculate the EoS below  $T_{ch}$  in the Boltzmann approximation of ideal multi-component hadron gas. In addition to standard HKM method we add now excluded volume  $v_0$  (equal for all hadrons) which may be important for baryon-rich systems, according to the following formula:

$$p(T, \{\mu_i\}) = \sum_i p_i^{\text{id}}(T, \{\mu_i - v_0 \cdot p\}) \quad (8)$$

the superscript *id* refers to ideal gas case. We solve this equation numerically, and obtain other thermodynamic quantities using general thermodynamic relations and the solution of Eq.(8).

We match energy and baryon number densities in both EoS at chemical freeze-out point, and minimize pressure difference there as well. We choose the excluded volume value  $v_0 = 0.2 \text{ fm}^3$  from the condition of the best matching. The corresponding energy and net baryon densities are  $\{\epsilon, n_B\} = \{0.4 \text{ GeV/fm}^3, 0.085 \text{ 1/fm}^3\}$  for  $E_{\text{Lab}} = 158 \text{ GeV}$  and  $\{\epsilon, n_B\} = \{0.34 \text{ GeV/fm}^3, 0.12 \text{ 1/fm}^3\}$  for  $E_{\text{Lab}} = 40 \text{ GeV}$  collisions, which correspond to the chemical freeze-out parameters shown above. The chosen excluded volume in chemically non-equilibrated ideal hadron gas thus mimics more complicated interactions happening in hadron matter in two-phase model before chemical freeze-out.

### 2.3 Evolution

At the temperatures higher than  $T_{ch}$  the hydrodynamic evolution is related to the possible quark-gluon, mixed and hadron phases which are in chemical equilibrium with some baryonic chemical potential. The evolution is described by the conservation law for the energy-momentum tensor of perfect fluid:

$$\partial_\nu T^{\mu\nu}(x) = 0 . \quad (9)$$

Since in perfect hydrodynamics the entropy is conserved, the system evolves along trajectories shown in Fig.2.

At  $T < T_{ch}$  the system evolves as chemically non-equilibrated hadronic gas. The concept of the chemical freeze-out implies that afterwards only elastic collisions and resonance decays take place because of relatively small densities allied with a fast rate of expansion at the last stage. Thus, in addition to Eq.(9), the equations accounting for the particle number conservation and resonance decays are added. If one neglects the thermal motion of heavy resonances, the equations for particle densities  $n_i(x)$  take the form:

$$\partial_\mu(n_i(x)u^\mu(x)) = -\Gamma_i n_i(x) + \sum_j b_{ij}\Gamma_j n_j(x) \quad (10)$$

where  $b_{ij} = B_{ij}N_{ij}$  denote the average number of  $i$ -th particles coming from arbitrary decay of  $j$ -th resonance,  $B_{ij} = \Gamma_{ij}/\Gamma_{j,tot}$  is branching ratio,  $N_{ij}$  is a number of  $i$ -th particles produced in  $j \rightarrow i$  decay channel. Eqs.(9) and Eqs.(10) are solving simultaneously with calculation of the EoS,  $p(x) = p(\epsilon(x), \{n_i(x)\})$  at each point  $x$ .

#### 2.4 System's decoupling and spectra formation

During the matter evolution, in fact, at  $T \leq T_{ch}$ , hadrons continuously leave the system. Such a process is described by means of the emission function  $S(x, p)$  which is expressed through the *gain* term for  $i$ -th sort of particles,  $G_i(x, p)$ , in Boltzmann equations and the escape probabilities [4,5]

$$S_i(x, p) = G_i(x, p)\mathcal{P}_i(x, p)$$

$$\mathcal{P}_i(x, p) = \exp\left(-\int_t^\infty ds R_{i+h}(s, \mathbf{r} + \frac{\mathbf{p}}{p^0}(s-t), p)\right).$$

For particle emission in the relaxation time approximation  $G_\pi \approx f_\pi R_{\pi+h} + G_{H \rightarrow \pi}$  where  $f_\pi(x, p)$  is the Bose-Einstein phase-space distribution,  $R_{i+h}(x, p)$  is the total collision rate of the particle, carrying momentum  $p$ , with all the hadrons  $h$  in the system in a vicinity of point  $x$  and the term  $G_{H \rightarrow i}$  describes an inflow of particles into phase-space point  $(x, p)$  due to the resonance decays. It is calculated according to decay kinematics with simplification that the spectral function of the resonance  $H$  is  $\delta(p^2 - \langle m_H \rangle^2)$ . The cross-sections of interacting particles in the hadronic gas, which determine the escape probabilities  $\mathcal{P}(x, p)$  and emission function  $S(x, p)$  via the collision rate  $R_{i+h}$ , are calculated in accordance with the UrQMD method [20]. The spectra and correlation functions are found from the emission function  $S$  in the standard way (see, e.g.,[4]).

### 3 Results and conclusions

The results for transverse mass spectra and interferometry radii are presented in Fig. 3 for the two SPS energies. The two fitting parameters: maximal initial energy density  $\epsilon_0$  and the initial transverse velocity (associated with parameter  $\alpha$ ) averaged over the energy profile  $\langle v_T \rangle$  are equal to  $\epsilon_0 = 5 \text{ GeV/fm}^3$  ( $\langle \epsilon \rangle = 3.5 \text{ GeV/fm}^3$ ) for  $E_{Lab}=40 \text{ AGeV}$  and  $\epsilon_0 = 8 \text{ GeV/fm}^3$  ( $\langle \epsilon \rangle = 5.6 \text{ GeV/fm}^3$ ) for  $E_{Lab}=158 \text{ AGeV}$  and  $\langle v_T \rangle = 0.196$  for both energies. As one can see the pion and kaon transverse mass spectra, their slopes as well as the absolute values

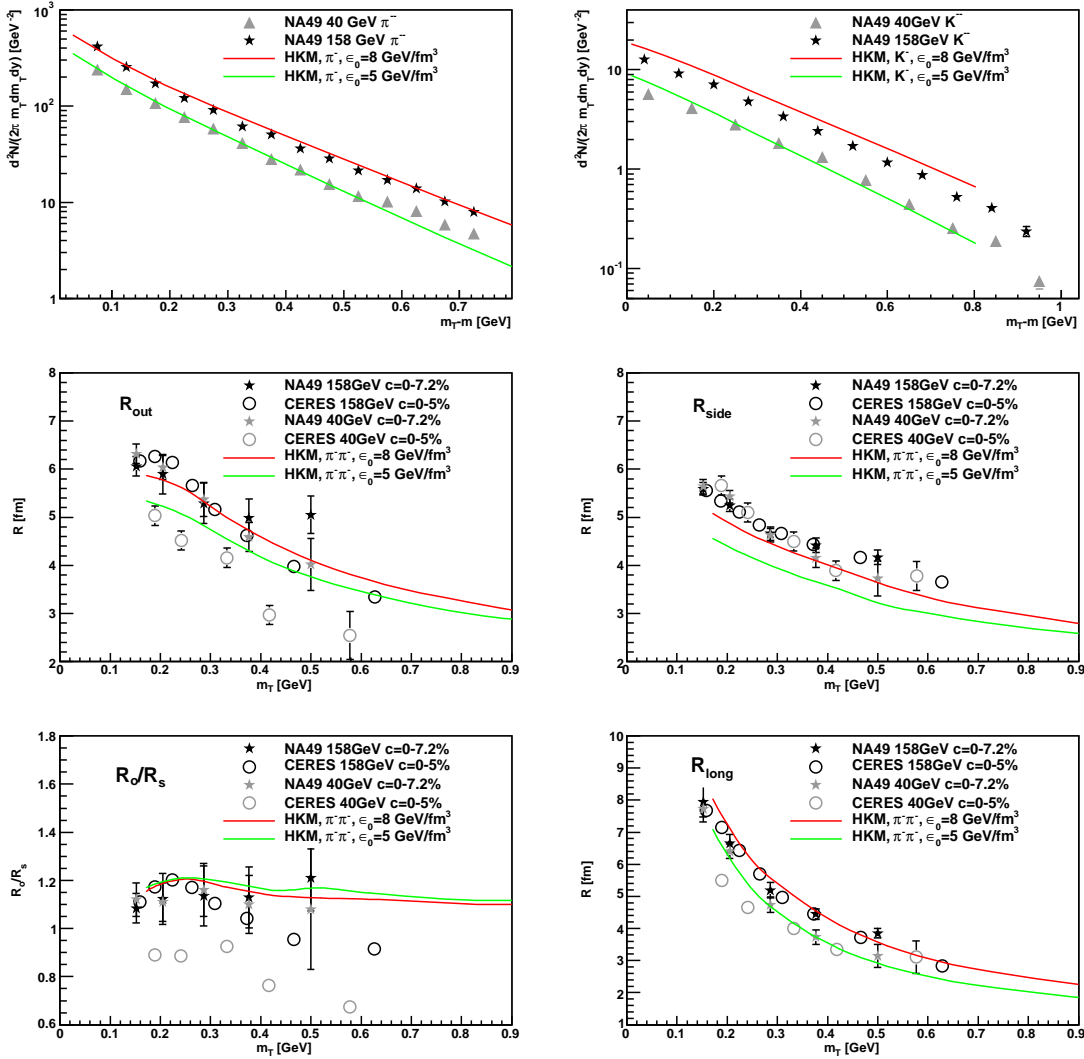


Fig. 3. Pion and kaon spectra (top), pion  $R_{out}$ ,  $R_{side}$  (middle),  $R_{long}$  and  $R_{out}/R_{side}$  ratio (bottom) as a function of transverse momentum at the given centrality. Experimental points for transverse spectra and interferometry radii are taken from [21] and [22,23], respectively.

are in a quite reasonable agreement with available experimental data [21].

A good agreement with experiments [22,23] is also observed for the longitudinal radius  $R_{long}$  for the both energies studied. The  $R_{out}$  and  $R_{side}$  interferometry radii are well reproduced for the top SPS energy including even the ratio  $R_{out}/R_{side}$  which is more sensitive to model parameters. For  $E_{lab} = 40$  AGeV there are some deviations of the calculated curves from experimental points which are more pronounced for the  $R_{out}/R_{side}$  ratio.

Summarizing, one can note that the hydrokinetic model can serve as the basic dynamical model also for low-energy collisions where the equation of state corresponding to the first order phase transition should be used rather than that with crossover transformation between quark-gluon and hadron matter. Such an EoS at large chemical potentials can be successfully constructed by matching the relativistic mean-field approximation for EoS at  $T > T_{ch}$  with ideal hadronic gas with hadron masses below 2.6 GeV including the excluded volume assumption at  $T < T_{ch}$ . This approach reasonably reproduces not only bulk properties of produced particles but also such delicate characteristics as interferometry radii. It is worthy to note that even at  $E_{lab} = 40$  AGeV the description of experimental data requires to take into account quark-gluon degrees of freedom in initial thermodynamic conditions. The HKM may be useful in predictions of collective observable in the energy considered in future FAIR and NICA experiments.

## Acknowledgments

We are thankful to P. Braun-Munzinger and D. Voskresensky for useful comments. The work was supported in part by the State Fund for Fundamental Researches of Ukraine, Agreement No F28/335-2009 and Russian Fund of Fundamental Researches, Agreement Ukr-f-a 09-02-90423 for the Bilateral project SFFR (Ukraine) RFFR (Russia) and by the DFG grant WA 431/8-1. The research is carried out within the scope of the EUREA: European Ultra Relativistic Energies Agreement (European Research Group: Heavy ions at ultrarelativistic energies) supported by SFFR and NASU.

## References

- [1] P.F. Kolb, P. Huovinen, U. Heinz and H. Heiselberg, Phys. Lett. B **500**, 232 (2001); U. Heinz and P. Kolb, Nucl. Phys. A **702**, 269 (2002).

- [2] The ALICE Collaboration, arXiv:1011.3914 [nucl-ex].
- [3] W. Florkowski, W. Broniowski, M. Chojnacki and A. Kisiel, Acta Phys. Polon. B **40**, 1093 (2009); W. Florkowski, W. Broniowski, M. Chojnacki and A. Kisiel, Nucl. Phys. A **830**, 821 (2009).
- [4] Yu.M. Sinyukov and S.V. Akkelin, Y. Hama, Phys. Rev. Lett. **89**, 052301 (2002).
- [5] S.V. Akkelin, Y. Hama, Iu.A. Karpenko and Yu.M. Sinyukov, Phys. Rev. C **78**, 034906 (2008).
- [6] Iu. Karpenko and Yu.M. Sinyukov, Phys. Rev. C **81**, 054903 (2010)
- [7] Iu.A. Karpenko and Yu.M. Sinyukov Phys. Lett. B **688**, 50 (2010).
- [8] A.S. Khvorostukhin, V.D. Toneev and D.N. Voskresensky, Nucl. Phys. A **791**, 180 (2007).
- [9] P. F. Kolb, J. Sollfrank, and U. W. Heinz, Phys. Lett. B **459**, 667 (1999); U. W. Heinz and H. Song, J. Phys. G **35**, 104126 (2008).
- [10] K. Werner, Phys. Rev. Lett. **98**, 152301 (2007).
- [11] Yu.M. Sinyukov, Acta Phys. Polon. B **37**, 4333 (2006); M. Gyulassy, Iu.A. Karpenko, A.V. Nazarenko and Yu.M. Sinyukov, Braz. J. Phys. **37**, 1031 (2007); J. Vredevoogd and S. Pratt, arXiv:0810.4325; S. Pratt, arXiv:0903.1469; Yu.M. Sinyukov, A.V. Nazarenko, Iu.A. Karpenko, Acta Phys. Polon. B **40**, 1109, (2009).
- [12] Yu.M. Sinyukov, Iu.A. Karpenko and A.V. Nazarenko, J. Phys. G: Nucl. Part. Phys. **35**, 104071 (2008).
- [13] D. Teaney, Phys. Rev. C **68** (2003) 034913.
- [14] R. P. G. Andrade, F. Grassi, Y. Hama, T. Kodama, and W. L. Qian, Phys. Rev. Lett. **101**, 112301 (2008).
- [15] A.S. Khvorostukhin, V.D. Toneev and D.N. Voskresensky, Nucl. Phys. A **813**, 313 (2008).
- [16] E.E. Kolomeitsev and D.N. Voskresensky, Nucl. Phys. A **759**, 373 (2005).
- [17] F. Becattini and J. Manninen, J. Phys. G: Nucl. Part. Phys. **35**, 104013 (2008); A. Andronic, P. Braun-Munzinger and J. Stachel, arXiv:0812.1186; arXiv:0901.2909.
- [18] [http://pdg.lbl.gov/2009/html/computer\\_read.html](http://pdg.lbl.gov/2009/html/computer_read.html).
- [19] A. Andronic, P. Braun-Munzinger and J. Stachel, Acta Phys. Polon. B **40**, 1005 (2009); A. Andronic, P. Braun-Munzinger and J. Stachel, arXiv:0911.4931 [nucl-th].
- [20] M. Bleicher et al., J. Phys. G: Nucl. Part. Phys. **25**, 1859 (1999).

- [21] S. V. Afanasiev et al. (The NA49 Collaboration), Phys. Rev. C **66**, 054902 (2002).
- [22] C. Alt et al. (The NA49 Collaboration), Phys.Rev. C **77**, 064908 (2008).
- [23] D. Antończyk, Acta Phys. Polon. B **40**, 1137 (2009).